Research on Residual Stress Measurement of Magnesium Alloy Cabin Castings

YIN Lan[1,2], FANG Yu[4], WU Yunxin[1,2,3], ZHANG Tao[1,2], LI Chengxin[4], GONG Hai[1,2]

(1.Light Alloy Research Institute, Central South University, Changsha 410083, Hunan, China; 2.State Key Laboratory of High Performance Complex Manufacturing, Central South University, Changsha 410083, Hunan, China; 3.College of Mechanical and Electrical Engineering, Central South University, Changsha 410083, Hunan, China; 4.Shanghai Spaceflight Precision Machinery Institute, Shanghai 201600, China)

Abstract: Owing to the nonuniform wall thickness and complex internal structure, the measurement of the residual stress on magnesium alloy cabin castings is complex and difficult extremely, and thus seldom research has focused on the residual stress of magnesium alloy castings. In this paper, the blind-hole method, the X-ray diffraction (XRD) method, and the contour method are used to conduct comprehensive and systematic residual stress tests for a magnesium alloy cabin casting. The results show that the residual stress on the surface of the casting obtained by the blind-hole method is between −20.03 MPa and −71.03 MPa, the residual stress obtained by the XRD method is between −26.01 MPa and −87.11 MPa, while the residual stress obtained by the contour method is between −45.89 MPa and 76.87 MPa. The study can lay a basis for the subsequent research of magnesium alloy cabin castings, and provide a reference for the residual stress test of magnesium alloy castings.

Key words: magnesium alloy; residual stress; XRD method; blind-hole method; contour method

Chinese Library Classification: TB302 **Document code:** A **DOI:** 10.19328/j.cnki.2096-8655.2022.01.004

0 Introduction

Mg-10Gd-3Y-0.3Zr (GW103K) magnesium alloy is a rare earth magnesium alloy. It has the characteristics such as high strength, good heat resistance, light weight, and good casting, and has been widely applied to the large and complex casting parts in the aerospace field[1]. However, such phenomena as cracking, deformation, and dimensional deviation may occur in the castings, owing to the inevitable existence of residual stress. The residual stress seriously affects the strength of the component materials and their related performance, and should be accurately monitored. Therefore, the accurate test of casting residual stress is of great significance for improving the utilization rate of magnesium alloy and improving the quality of aviation aircraft[2].

Many residual stress test methods have been developed[3]. According to the damage degree of test pieces, the test methods can be divided into destructive testing methods and non-destructive testing methods. Commonly used destructive testing methods include the blind-hole method, the crack compliance method, and the profile method, while commonly used non-destructive testing methods include the XRD method, the neutron diffraction method, and the ultrasonic method. LI et al.[4] measured the welding residual stress of beam-column joints with the blind-hole method, and obtained data consistent with the simulation results. MAARTEN et al.[5] used the crack compliance method to determine the

Received date: 2021-09-15; **Revised date:** 2021-11-15

Author: YIN Lan (1986—), female, Ph. D., lecturer. Her main research interests include component stress modeling analysis and characterization.

Corresponding author: WU Yunxin (1963—), male, Ph. D., professor. His main research interests include theory and application of mechanical dynamics, residual stress detection and reduction of materials and components.

residual stress of the bottom plate and welding specimens. XIE et al.[6] combined the profile method and the X-ray diffraction method to measure the quenching residual stress of the aluminum alloy component, and accurately described the quenching residual stress field of the T-shaped component. LIU et al.[7] used the X-ray diffraction method to measure the residual stress of the tube blank with a large deformation free compression diameter, and obtained data consistent with the theoretical analysis results. Compared with the X-ray diffraction method, the neutron diffraction method has stronger penetrating power and can be used to measure the residual stress inside a larger solid material. However, the neutron diffraction stress test equipment is expensive, and the running time is long. Therefore, it is less used in China now. FIORI et al.[8] determined the three-dimensional distribution law of residual stress for automobile steel gears with the neutron diffraction method. WANG et al.[9] proposed an improved ultrasonic method to measure the plane stress in orthotropic materials.

The research time of magnesium alloy as a structural material is relatively short, and the research on its residual stress is still in its infancy[10-11]. In this paper, the blind-hole method, the X-ray diffraction method, and the profile method are used to test the residual stress of a magnesium alloy cabin casting, respectively. The obtained results can provide an experimental basis for the subsequent heat treatment and machining process for magnesium alloys and provide some reference for the residual stress testing technology.

1 Blind-hole method

1.1 Basic principle of the blind-hole method and the strain release factor

The blind-hole method was first proposed by MATHAR in 1934, and gradually improved by SOETE and other scholars. In 1981, American Society for Testing Materials (ASTM) included the blind-hole method in the ASTM E837-81 standard named as Standard Test Method for Residual Stress Determination by the Borehole Strain Method. The blind-hole method was also published in the national standard GB/T 31310—2014 in China[12]. The measurement principle is simple. Firstly, paste the strain gage on the surface of the workpiece. Secondly, drill a hole in the center of the strain gage to break the original residual stress field, and release the residual stress of the blind-hole accessories. Thirdly, measure the strain change. Finally, calculate the residual stress according to the relevant principles of elasticity[13-15].

Before the residual stress is released, the A and B coefficients are calculated according to the calibration test. A unidirectional stress field is applied to the specimen so that one direction of the strain gage is parallel to the direction of the applied stress. Make the maximum principal stress σ applied to the strain gage be equal to the stress σ applied by the external load, and then drill the hole. After the drilling is completed, measure the strain of the strain gage. Then, the values of A and B can be obtained by

$$\begin{cases} A = \left(\varepsilon_1 + \varepsilon_3\right) / 2\sigma \\ B = \left(\varepsilon_1 - \varepsilon_3\right) / 2\sigma \end{cases} \tag{1}$$

where A and B are the stress calibration constants, ε_1 and ε_3 are the strain values, and σ is the stress. In order to accurately measure the residual stress under different stress levels, the calibration stresses are, respectively, equal to $0.3\sigma_s$, $0.5\sigma_s$, and $0.7\sigma_s$, where σ_s is the yield stress of the material. Then, A and B are graded, by which the errors generated by the plastic deformation of the hole edge can be avoided.

Generally speaking, the surface residual stress measured by the blind-hole method is a plane stress state, and its two-way principal stress and directional angle are unknown. Therefore, it is necessary to use three-way strain rosettes to measure the stresses. The low-speed drilling method is adopted in this article, with which the residual stress values of the measuring point can be calculated by

$$\begin{cases} \sigma_1 = C_1(\Delta\varepsilon_1 + C_2\Delta\varepsilon_3) \\ \sigma_3 = C_1(\Delta\varepsilon_3 + C_2\Delta\varepsilon_1) \end{cases} \tag{2}$$

where σ_1 and σ_3 are the stress values in the directions of the strain gages 1 and 3, corresponding to the axial and circumscribed stresses in this paper, respectively. $\Delta\varepsilon_1$ and $\Delta\varepsilon_3$ are the strain values in the directions of the strain gages 1 and 3, respectively. $C_1 = (A+B)/(4AB)$, and $C_2 = \frac{(B-A)}{(A+B)}$, in which A and B are the stress calibration coefficients.

1.2 Experimental procedure

The material is magnesium alloy. The test instruments include HK21B drilling device, YE2533 program-controlled static strain gauge, multimeter, etc. The strain rosette is TJ120-1.5-ϕ1.5, type A. The measurement procedure mainly consists of attaching the strain gage, drilling the hole, and recording the readings of the strain gauges. The drilling procedure of the measuring points is shown in Fig. 1. The marking diagram of the measuring points on a workpiece is shown in Fig. 2. In order to understand the residual stress distribution on the surface of a magnesium alloy cabin casting, three paths are considered, i.e., Path L1, Path L2, and Path L3, as shown in Fig. 2.

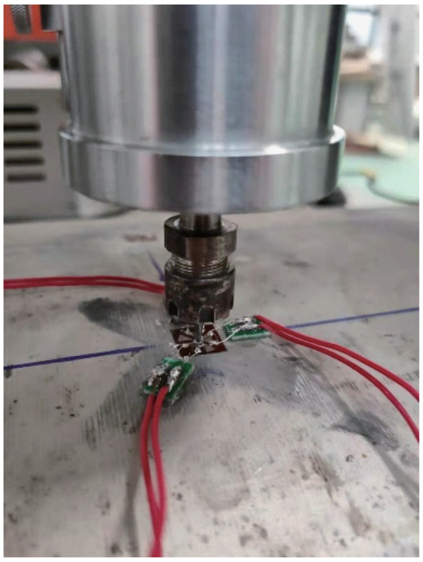

Fig. 1 Picture of specimen point drilling

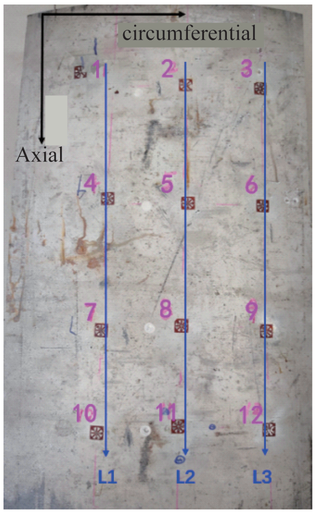

Fig. 2 Marking diagram of the measuring points

1.3 Results and analysis

During the test, the first direction of the strain gage corresponds to the axial direction and the third direction corresponds to the circumscribed direction (see Fig. 2). The residual stress test results of the blind-hole method are shown in Tab. 1. As can be seen from Tab. 1, the surface stress of the magnesium alloy cabin casting is compressive, and the value is between 20.03 MPa and 71.03 MPa. The stress evolutions of different paths, i.e., (a) L1, (b) L2, and (c) L3, are shown Fig. 3. The analysis results of the test results shown in Fig. 3 are as follows.

Tab. 1 Results of the blind-hole method

No.	Axial residual stress/MPa	Circumferential residual stress/MPa
1	−20.41	−25.15
2	−42.64	−58.47
3	−54.16	−71.03
4	−30.38	−37.77
5	−50.10	−56.57
6	−51.32	−68.31
7	−20.03	−36.21
8	−35.55	−57.04
9	−30.64	−45.66
10	−55.76	−65.35
11	−27.03	−30.38
12	−20.72	−34.47

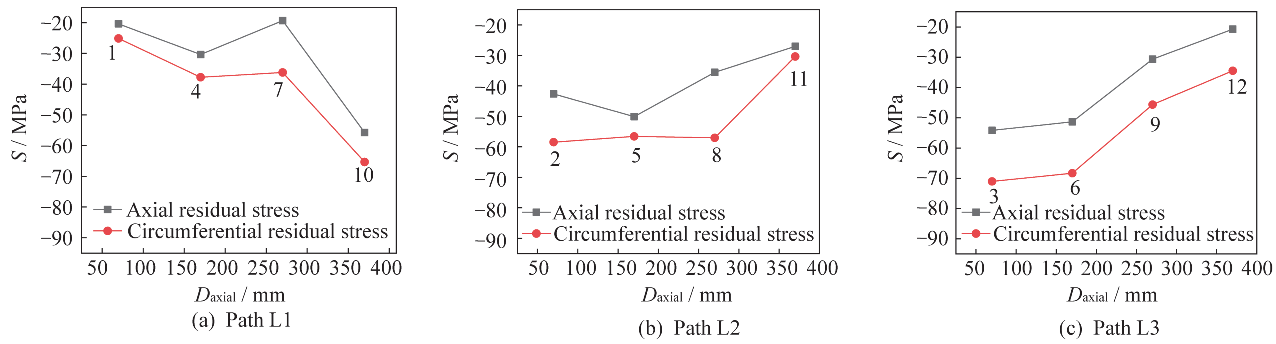

Fig. 3 Residual stress evolutions of different paths

1) The axial residual stress and the circumscribed residual stress have roughly the same variation trend, but the absolute value of the circumscribed residual stress is slightly larger than that of the axial residual stress.

2) The stress of Path L1 from Point 1 to Point 10 basically shows an increasing trend. This is because there are bars on the inner surface of the cabin casting at Points 4, 7, and 10 and the stress gradually increases with the increase in the wall thickness.

3) The residual stress of Path L2 is basically stable. This is because there is an internal hole at Point 11 and the wall thickness is thinner, which make the residual stress value become smaller.

4) On Path L3, there is a stiffened rib plate inside the cabin. The residual stresses of the first two measuring points are larger than those of Paths L1 and L2. This is because the internal structure of Point 9 is complex, the cold iron is added during casting, and thus the residual stress can be controlled.

2 X-ray diffraction method

2.1 Theory of the XRD method

Among all kinds of non-destructive residual stress testing methods, the XRD method is the most widely used one in the field of material science and mechanical engineering at present. The test principle is as follows: when there is residual stress inside a material, the material lattice spacing will change, which will results in a certain strain on the microscopic scale. X-ray can emit diffraction when it penetrates a metal lattice. The XRD method measures the residual stress value by measuring the change of the material lattice spacing[16]. Based on the $\sin^2\psi$ method, the stress σ_φ can be expressed as follows[17-18]:

$$\sigma_\varphi = \frac{1}{(1/2)S_2} \cdot \frac{\partial \varepsilon_{\varphi\psi}}{\partial \sin^2\psi} \tag{3}$$

where ϕ is the angle between the normal projection of the diffracted crystal plane and a specified direction on the specimen plane, ψ is the angle between the normal of the sample and the normal of the diffracting lattice plane, $\varepsilon_{\phi\psi}$ is the strain in the direction defined by ϕ and ψ, and $(1/2)S_2$ is the X-ray elasticity constant of the lattice planes $\{hkl\}$.

The lattice strain $\varepsilon_{\phi\psi}$ can be expressed by the interplanar spacing as follows:

$$\varepsilon_{\phi\psi} = \frac{d_{\phi\psi} - d_0}{d_0} \tag{4}$$

where d_0 and $d_{\phi\psi}$ represent the interplanar distances of the lattice planes $\{hkl\}$ of an unstrained specimen and a strained specimen, respectively. Both d_0 and $d_{\phi\psi}$ satisfy

$$2d_0 \sin\theta_0 = n\lambda \tag{5}$$

$$2d_{\phi\psi} \sin\theta_{\phi\psi} = n\lambda \tag{6}$$

where λ is the wavelength of the incident X-rays, and θ_0 and $\theta_{\phi\psi}$ represent the Bragg angles of the lattice planes $\{hkl\}$ of an unstrained specimen and a strained specimen, respectively.

2.2 Experimental procedure

When the residual stress of a magnesium alloy sample is determined by the XRD method, it is difficult to test the magnesium alloy sample because the

XRD signal of the magnesium alloy material is not strong enough. However, as a nondestructive testing method of residual stress, the XRD method has an important reference function to judge the residual stress. Therefore, residual stress XRD tests are carried out on magnesium alloy samples to explore the best diffraction parameters. To obtain the residual stress on the surface of the cabin casting, using the Proto device that is convenience and efficiency. Experimental results show that X-radiation source using Co targets can acquire great results, and the detailed parameter settings of the X-ray diffractometer are shown in Tab. 2.

Tab. 2 X-ray measurement parameters for the residual stress tests with the XRD method

Device	Proto
X-ray generator power	20 kV·4 mA
X-radiation source	Co $K\alpha$ (λ=0.179 02 nm)
Experimental time	8 s
Experimental number	10
Angle	$\beta=25^{\circ}$, $\phi=(0^{\circ}$ and $90^{\circ})$
Young's modulus	45 GPa
Poisson's ratio	0.29

Test points and Path L4 are shown in Fig. 4, which are selected from the measurement point accessories of the blind-hole method. The surface is treated with electrolytic polishing. In the stress test with the X-ray diffraction method, the axial and circumferential directions are consistent with those of the blind-hole method. The test process is shown in Fig. 5.

2.3 Results and analysis

When the XRD method is used to test the residual stress of the magnesium alloy cabin casting, 4 points are selected along the axial direction to form Path L4. The test results are shown in Tab. 3. It can be seen from Tab. 3 that the surface stress of the workpiece is compressive and the residual stress value is between 26 MPa and 88 MPa.

The residual stress evolutions of Path L4 are shown in Fig. 6. It can be seen from Fig. 6 that the

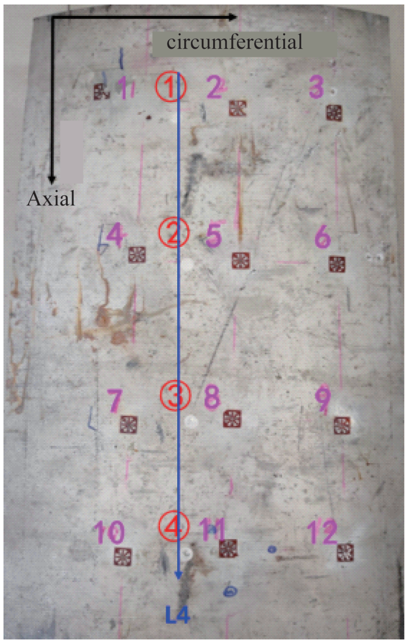

Fig. 4 Test points and Path L4

Fig. 5 Measurement setup with Proto

Tab. 3 Results of the X-ray diffraction method

No.	Axial residual stress/MPa	Circumferential residual stress/MPa
①	−48.52	−43.61
②	−26.01	−46.01
③	−39.92	−64.81
④	−87.11	−86.86

axial stress is slightly smaller than the circumferential stress, and the value of the stress shows an increase trend as the axial distance increases. In particular, the residual stress of Point ③ increases because it is at the connection between the upper plate and the shell, while the residual stress of Point ④ is the largest since Point ④ is at the connection between the side wall of the rudder shaft hole and the shell where the wall thickness is the thickest.

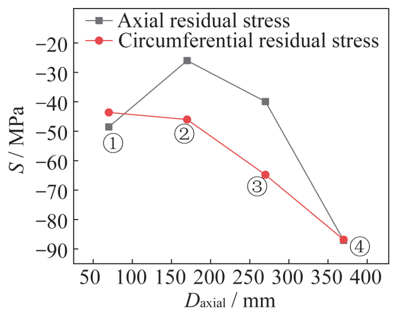

Fig. 6 Residual stress evolutions of Path L4

Comparing the test results of the XRD method and the blind-hole method, one can see that the stress value obtained by the XRD method is slightly larger than the stress value obtained by the blind-hole method. The detection depth of the XRD method is on the order of 10 microns, while the detection depth of the blind-hole method is on the order of millimeters. There is a gradient in the stress field, and there will be some differences in the detection results of the two methods. Besides, the detection error of the XRD method instrument is about 10 MPa, while the systematic error of the blind-hole method involves many factors and is generally more than 10 MPa. Therefore, the surface residual stresses measured by the blind-hole method and the XRD method are equivalent to each other, which can basically confirm each other.

3 Contour method

3.1 Theory of the contour method

In this paper, the contour method is used to test the residual stress cloud diagram of the circumferential section of the magnesium alloy cabin casting. The contour method was proposed by Prime in 2001. It mainly combines the finite element method and the stress relief technology to test the internal stress of a component[19]. The test principle is derived from the Bueckner superposition principle[20]. Firstly, cut the test piece along a certain plane. Secondly, deform the cutting surface profile generated by the stress release. The deformation profile is assumed to be caused by the elastic release of the residual stress. Thirdly, measure the deformation profile of the cutting surface accurately, and process the measured profile data. Finally, use the fitting results as the basic data of the finite element model, and obtain the stress distribution inside the component perpendicular to the cutting plane through elastic calculation[21].

3.2 Experimental procedure

Firstly, the workpiece is divided into two halves by Suzhou Sanguang DK7625P slow-moving wire cutting machine. The average wire speed is set as 1 $\mathrm{mm \cdot min^{-1}}$, and the cutting wire is a copper wire with ϕ0.25 mm. In order to ensure the hypothetical conditions of plane cutting, the two sides of the cutting surface are clamped symmetrically in the experiment. Secondly, the obtained cutting plane is measured by using the three-coordinate measuring machine. The distance between the measuring points is 3 mm×3 mm, and the error is 0.1 μm. The cutting surface of the workpiece is shown in Fig. 7.

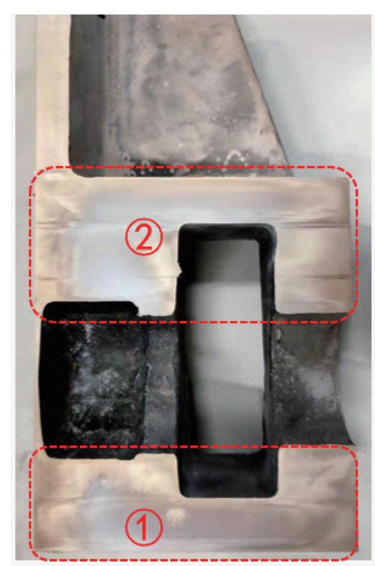

Fig. 7 Cutting surface of the workpiece

When a three-coordinate instrument is used to measure the contour, since the test piece cannot maintain the absolute level, the result of the measurement contour will be superimposed on the original inclined surface. Contour envelope processing can eliminate this error. In addition, the contour will be deformed at the sudden change of the cutting current, and smooth contour fitting can reduce this error. Contour fitting can also eliminate some measurement errors.

In this paper, the final contour data interpolated on the node coordinates are obtained by Matlab software, and the Gaussian mixture model is used for the fitting. Areas ① and ② are divided into 5×5 grids. The final contour data are shown in Fig. 8. It can be seen from Fig. 8 that the contour of Area ① is relatively smooth, while there is a higher peak value on the contour of Area ②. The existence of the peak value in Fig. 8(b) is because of the short circuit and wire breakage during the slow wire cutting process.

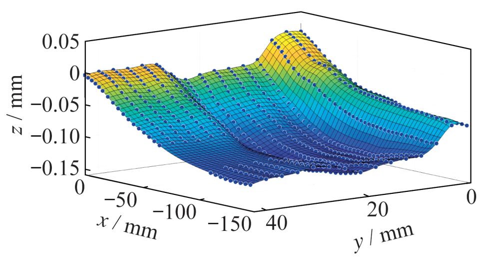

(a) Area ①

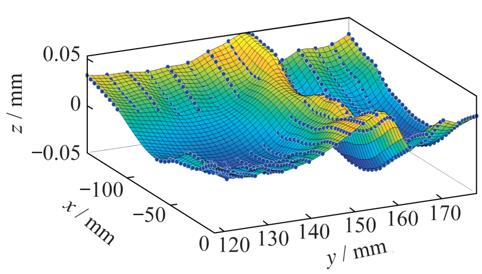

(b) Area ②

Fig. 8 Contour data

3.3 Results and analysis

The specimen model is established in ABAQUS, and the above processed contour data are inverted as the displacement boundary condition and loaded into the model. The Poisson's ratio is 0.29, and the elastic modulus is 45 GPa. The mesh element is determined to be a hexahedral eight-node one. The normal stress cloud diagram of the cross-section is shown in Fig. 9. It can be seen from Fig. 9 that the maximum tensile stress exists in the core of the thicker part of the cross-section. Besides, compressive stress exists in the outside part of the cross-section (boundary), while tensile stress exists in the inside part of the cross-section. In order to further study the distribution of the residual stress, four paths are taken in Area ① and Area ②, respectively, as shown in Fig. 10.

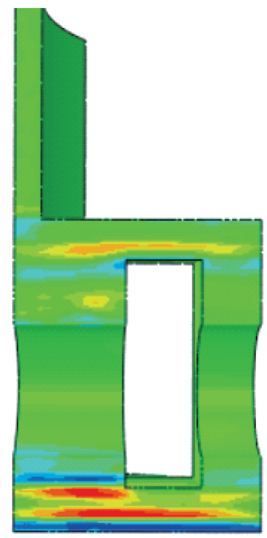

Fig. 9 Normal stress cloud of the cross-section

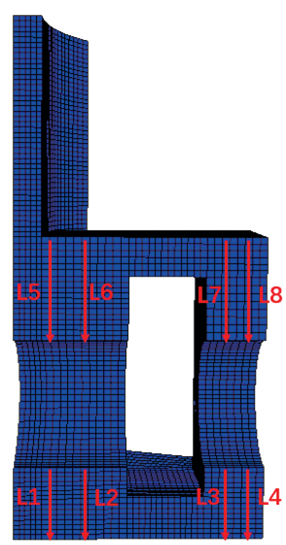

Fig. 10 Path diagram

The stress distributions of Areas ① and ② are shown in Fig. 11. Excluding the error of the contour method boundary, the stress in Area ① is roughly internally tensioned and externally compressed. It presents a bimodal stress distribution similar to that of a thick plate. Moreover, the maximum tensile stress is 76.87 MPa, and the maximum compressive stress is 45.89 MPa.

In addition, the radial wall thickness of the two paths on the left is thicker than that on the right. During the cooling process, the temperature difference between the surface and the core generates larger residual stress, which makes the residual stress value of the left path slightly larger than that of the right one. In Area ②, the stress distribution presents a bimodal shape, the maximum tensile stress is 53.21 MPa, and the maximum compressive stress is 23.18 MPa.

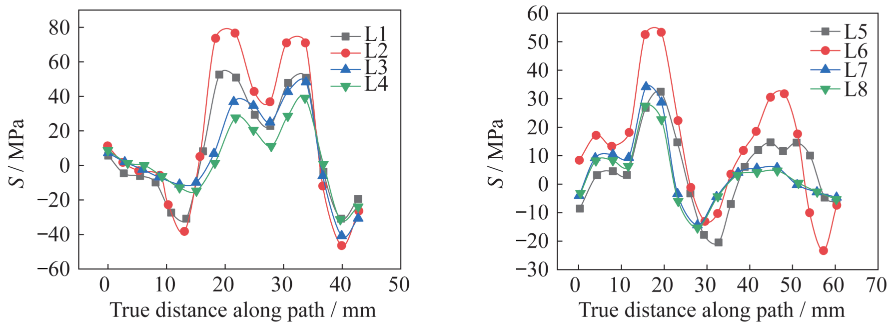

(a) Stress of Area ①　(b) Stress of Area ②

Fig. 11　Stress distributions of different paths in Areas ① and ②

4　Conclusions

In this paper, the residual stress in a magnesium alloy cabin casting is detected with the blind-hole method, the X-ray diffraction method, and the contour method, respectively. The residual stresses on the surface, near surface, and internal cross-section of the magnesium alloy cabin casting are detected. The specific conclusions are as follows:

1) The test results with the blind-hole method show that the surface stress of the magnesium alloy cabin casting is compressive, and its value is between 20.03 MPa and 71.03 MPa. The stress will be relatively larger when the wall thickness increases. Moreover, there is a certain stress concentration at the connection between the rudder shaft orifice plate and the shell.

2) The test results of the X-ray diffraction method show that the residual stress on the outer surface of the magnesium alloy cabin casting is compressive, and its value ranges from 26.01 MPa to 87.11 MPa. The test results are comparable to those of the blind-hole method, and can be mutually verified.

3) It can be known from the test results of the contour method that there is a certain regularity in the internal residual stress of the magnesium alloy cabin casting. The results present a bimodal stress distribution similar to that of the thick plate. The stress is between −45.89 MPa and 76.87 MPa.

References

[1] JIANG C H, YANG C Z. Internal stress diffraction analysis[M]. Beijing: Science Press, 2013.

[2] WANG C C. Research status and prospects of residual stress testing and calibration methods[J]. Measurement Technology, 2021, 41(2): 56-63.

[3] STEINZIG M, TAKAHASHI T. Residual stress measurement using the hole drilling method and laser speckle interferometry, Part IV: measurement accuracy [J]. Experimental Techniques, 2003, 27(6): 59-63.

[4] LI W R, ZHANG G L, LIU Y F, et al. Simulation and experimental verification of welding residual stress of Q345B steel beam-column joints [J]. Journal of South China University of Technology (Natural Science Edition), 2019, 47(10): 114-123.

[5] MAARTEN R, RICHARD P, HENK S, et al. A combined experimental and numerical examination of welding residual stresses [J]. Journal of Materials Processing Technology, 2018, 261: 98-106.

[6] XIE G Z, WU Y X, GONG H, et al. Data processing

in residual stress measurement using contour method [J]. China Mechanical Engineering, 2017, 28(15): 1778-1783.

[7] LIU H, WANG L D, WANG X D, et al. Research on the residual stress of the large deformation of the tube blank during the free push compression [J]. China Mechanical Engineering, 2021, 32(11): 1354-1360.

[8] FIORI, F, GIRARDIN E, GIULIANI A, et al. Neutron and synchrotron non-destructive methods for residual stress determination in materials for industrial applications [M]// OLEG N S, DANIEL B M, SERGEY A F. Metallic materials with high structural efficiency. Dordrecht: Springer, 2004: 425-432.

[9] WANG W, ZHANG Y M, ZHOU Y F, et al. Plane stress measurement of orthotropic materials using critically refracted longitudinal waves [J]. Ultrasonics, 2019, 94: 430-437.

[10] LIAO H B, LI X G, MA M L, et al. Current research status and application on magnesium alloy of residual stress[J]. Material Reports, 2012, 26(23): 107-111.

[11] FAN Z Z, CHEN J Z, LU Z, et al. Research status and development trend of magnesium alloys [J]. Foundry, 2020, 69(10): 1016-1029.

[12] Determination of residual stress in metallic materials and borehole strain method: GB/T 31310—2014 [S]. Beijing: China Standards Press, 2014.

[13] SU L J, ZHOU G T, LIU H S. Calibration and plastic correction on strain release coefficients in welding residual stress measurement of LY12 aluminum alloy by blind-hole method[J]. Materials and Testing, 2016, 40(4):48-53.

[14] ZHANG T, WANG Z Y, LI X L. Experimental study on welding residual stress of T-joint steel plate [J]. Journal of Building Structures, 2018, 39(Suppl.2): 128-134.

[15] MA X M, OU Q Y. Numerical simulation for hole-drilling strain gage method applied on curved surface [J]. Journal of South China University of Technology, 2019, 47(12): 25-31.

[16] MOORE M G, EVANS W P. Mathematical correction for stress in removed layers in X-ray diffraction residual stress analysis [J]. SAE Transactions, 1958, 66: 340-345.

[17] Non-destructive testing X-ray stress determination method: GB/T 7704—2017 [S]. Beijing: China Standards Press, 2017.

[18] ZHANG Z W, FENG YF, TAN Q, et al. Residual stress distribution in Ni-based superalloy turbine discs during fabrication evaluated by neutron/X-ray diffraction measurement and thermomechanical simulation [J]. Materials & Design, 2019, 166: 107603.

[19] PRIME M B, GONZALES A R. Proceedings of the sixth international conference on residual stresses [R]. Oxford: IOM Communications Ltd, 2000: 617-624.

[20] PRIME M B. Cross-sectional mapping of residual stresses by measuring the surface contour after a cut [J]. Journal of Engineering Materials and Technology, 2001, 123(2):162-168.

[21] PRIME M B, NEWBORN M A, BALOG J A. Quenching and cold-work residual stresses in aluminum hand forgings: contour method measurement and FEM prediction [J]. Materials Science Forum, 2003, 426-432(1): 435-440.